ISSN (Print) 1226-1750
ISSN (Online) 2233-6656
Journal of Magnetics 28(1), 72-76 (2023) https://doi.org/10.4283/JMAG.2023.28.1.072

Influence of V_2O_5 Addition on the Magnetic Properties of Li-Zn Ferrites

M. Samir Ullah[1]*, Sm. Rubayatul Islam[1], M. Atikul Islam[2], M. Hassan[1], M. Firoz Uddin[1], and M. Mizanur Rahman[2]

[1]*Department of Physics, Bangladesh University of Engineering and Technology, Dhaka-1000, Bangladesh*
[2]*Department of Physics, University of Dhaka, Dhaka-1000, Bangladesh*

(Received 1 August 2022, Received in final form 23 December 2022, Accepted 3 January 2023)

The structural property, bulk density and porosity of V_2O_5 (0.0, 0.4, 0.8 and 1.2 wt.%) added Li-Zn ferrites are observed along with the surface morphology. The samples have been prepared by the solid-state reaction technique and sintered at 1050 °C. The X-ray diffraction patterns of the prepared samples have shown the single phase cubic spinel structure. A microstructural study demonstrates that the grain size increases up to 0.8 wt.% V_2O_5 and slightly decreased thereafter for 1.2 wt.% V_2O_5 addition. The saturation magnetization value increases from 44.0 to 50.3 emu/g as the V_2O_5 content increases up to 0.8 wt.%. The decrease of magnetization for 1.2 wt.% V_2O_5 content is apparent and it is found to be 47.3 emu/g. This may be related to the dilution effect with the excess of non-magnetic V_2O_5. It is also observed that the value of initial permeability increases up to 0.8 wt.% V_2O_5.

Keywords : spinel ferrites, V_2O_5 addition, microstructure, magnetization, complex permeability

1. Introduction

Li-Zn spinel-type of mixed ferrites are ferrimagnetic materials that are used in high-density recording media, transformer cores and microwave devices in electronic industries due to their low cost, moderate saturation magnetization, high mechanical strength, chemical stability, and low dielectric loss [1-7]. There are different types of oxide such as V_2O_5, Bi_2O_3, MnO_2, MoO_3 and Nb_2O_5 have been used as an additive as a sintering aid in order to promote the grain growth and modify the microstructure which can influence the electric as well as the magnetic properties of the ferrites materials [8-13]. Usually, spinel ferrites are required high sintering temperature using solid-state reaction method in order to obtain good homogeneity and densification of the materials [14]. However, abnormal grain growth or discontinuous grain growth appears at higher sintering temperature, which can deteriorate the electromagnetic properties of the spinel ferrites. It is seen that V_2O_5 plays a significant role as the sintering aids (low melting point, T_m ~ 670 °C) which can increase the densification of the samples [15, 16]. The high magnetic permeability plays a crucial role in magnetic softening of the spinel ferrites from the application point of views. In this regard, it is expected that V_2O_5 can play a significant role as the sintering aids in order to improve the mass transport mechanism and densification of the Li-Zn ferrites samples. Therefore, it is interesting to investigate in detail the effect of V_2O_5 addition on the structural and magnetic properties of Li-Zn ferrites having the compositions $Li_{0.25}Zn_{0.50}Fe_{2.25}O_4 + xV_2O_5$ (where x = 0.0, 0.4, 0.8 and 1.2 wt.%).

*Corresponding author: Tel: +8801782069938
Fax: +88-9665613, e-mail: samirullah@phy.buet.ac.bd

2. Experimental

In order to prepare of Li-Zn ferrites, Li_2CO_3, ZnO, and Fe_2O_3 of high purity powders were used as starting materials. These powders were weighed with appropriate ratio and mixed thoroughly, and milling in a mortar-pestle for 5 h. Then the mixed powder was pre-sintered at 750 °C for 3 h. The calcined powders were mixed with different proportions of V_2O_5 (0.4, 0.8, 1.2 wt.%). Then V_2O_5 added Li-Zn ferrites samples were pressed in a hydraulic press to form disc and toroid shaped samples. Finally, the samples were sintered at 1050 °C in the air for 3 h. The X-ray diffraction (XRD) measurement was performed at room temperature in the 2θ range of 10 to 80° with Cu-K_α radiation. The characterization of the surface morphology of the samples had been studied with the field emission scanning electron microscopy (FESEM: JSM-7600F, JEOL). The magnetic properties such as hysteresis loop and saturation magnetization were observed at room temperature using a quantum design physical property measurement system (PPMS). The complex magnetic permeability of the toroid-shaped samples was measured by an impedance analyzer (WAYNE KERR 6500B).

3. Results and Discussion

Fig. 1 depicts the XRD patterns of V_2O_5 (0.0, 0.4, 0.8 and 1.2 wt.%) added Li-Zn ferrites. It is observed that the characteristic peaks of (111), (220), (311), (222), (400), (422), (511), and (440) fundamental reflection planes are found for all the samples, which have been confirmed to single-phase cubic spinel structure [17]. In addition, there has not been observed any diffraction peak of V_2O_5 which indicates that the involvement of V_2O_5 additive has no

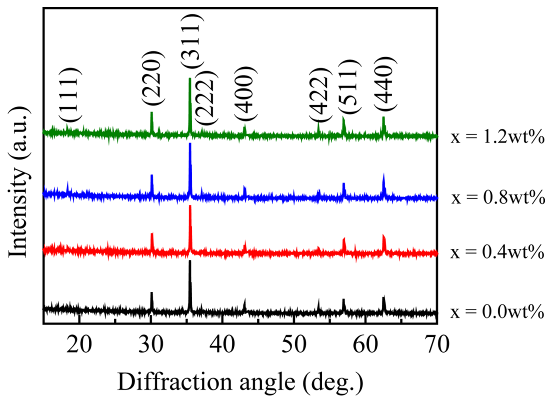

Fig. 1. (Color online) XRD patterns of V_2O_5 added Li-Zn ferrites sintered at 1050 °C.

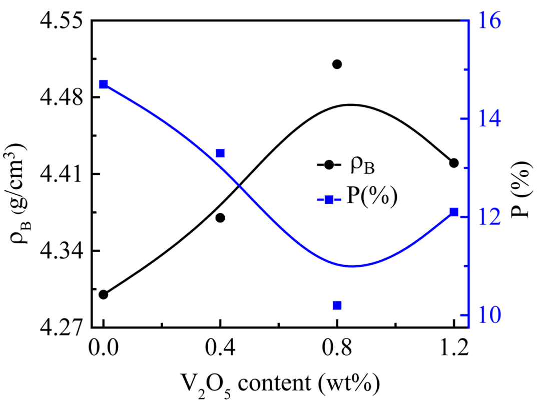

Fig. 2. (Color online) Variation of ρ_b and P (%) with different V_2O_5 contents sintered at 1050 °C.

influence on the crystal structure. The bulk density (ρ_B) and porosity (P%) of the studied samples are shown in Fig. 2. It is found that ρ_B increases with the increase of V_2O_5 content up to 0.8 wt.% and afterwards it decreased for 1.2 wt.% V_2O_5. While the porosity of the samples decreased with the addition of V_2O_5 contents, which could be attributed to the role of V_2O_5 as a sintering aid to enhance the densification of the samples from 4.30 g/cm^3 (for x = 0.0 wt.% V_2O_5) to 4.51 g/cm^3 (for x = 0.8 wt.% V_2O_5). However, P% increased for x = 1.2 wt.% V_2O_5 which may be related to the subsequent decrease of density of the sample.

The FESEM images of V_2O_5 (0.0, 0.4, 0.8 and 1.2 wt.%) added Li-Zn ferrites along the grain size distribution (histograms) are presented in Fig. 3. It can be seen that the grain growth of the studied samples strongly depends on the V_2O_5 addition. The average grain sizes vary from 5.3 (for x = 0.0) to 7.7 μm (for x = 0.8 wt.% V_2O_5). The increase of grain growth could be attributed to the formation of the liquid phase of V_2O_5 additive at the sintering process, which can accelerate grain growth along with densification of the samples [18]. However, the grain size was found to reduce for x = 1.2 wt.% V_2O_5. This decrease of grain size might be related to the excess addition of V_2O_5 which can hinder the grain growth [19]. As a consequence, irregular and inhomogeneous shaped grains have been observed at x = 1.2 wt.% V_2O_5. Fig. 4 shows the variation of the magnetization (M) with the applied magnetic field strength (H) at room temperature. The M-H curve clearly demonstrates the saturation magnetization states of the studied samples that indicate their ferrimagnetic nature. It is also observed that the samples have shown typical magnetic hysteresis behaviour. The variation of the saturation magnetization (M_s) with different amounts of V_2O_5 content is presented in Fig. 5. The value of M_s of Li-Zn ferrites (for 0.0 wt.% V_2O_5) is 44.0 emu/g. This is relatively low as compared with the other samples, which may be related to smaller grains caused by a low sintering temperature. M_s increases from 44.0 to 50.3 emu/g with increasing V_2O_5 content up to 0.8 wt.% due to grain growth and reduction of pores. This is happening due to the role of V_2O_5 as a sintering aid to enhance the densification of the samples along with larger grains resulting in a reduced inter-particle distance and a less number of magnetic free poles [20]. This is consistent with the microstructural feature. The relation between the grain growth and the magnetization of the sample demonstrates that the grain growth along with the densification of the samples can play a significant role in order to influence the magnetization of the Li-Zn ferrites. However, the value of M_s is found to deteriorate for 1.2

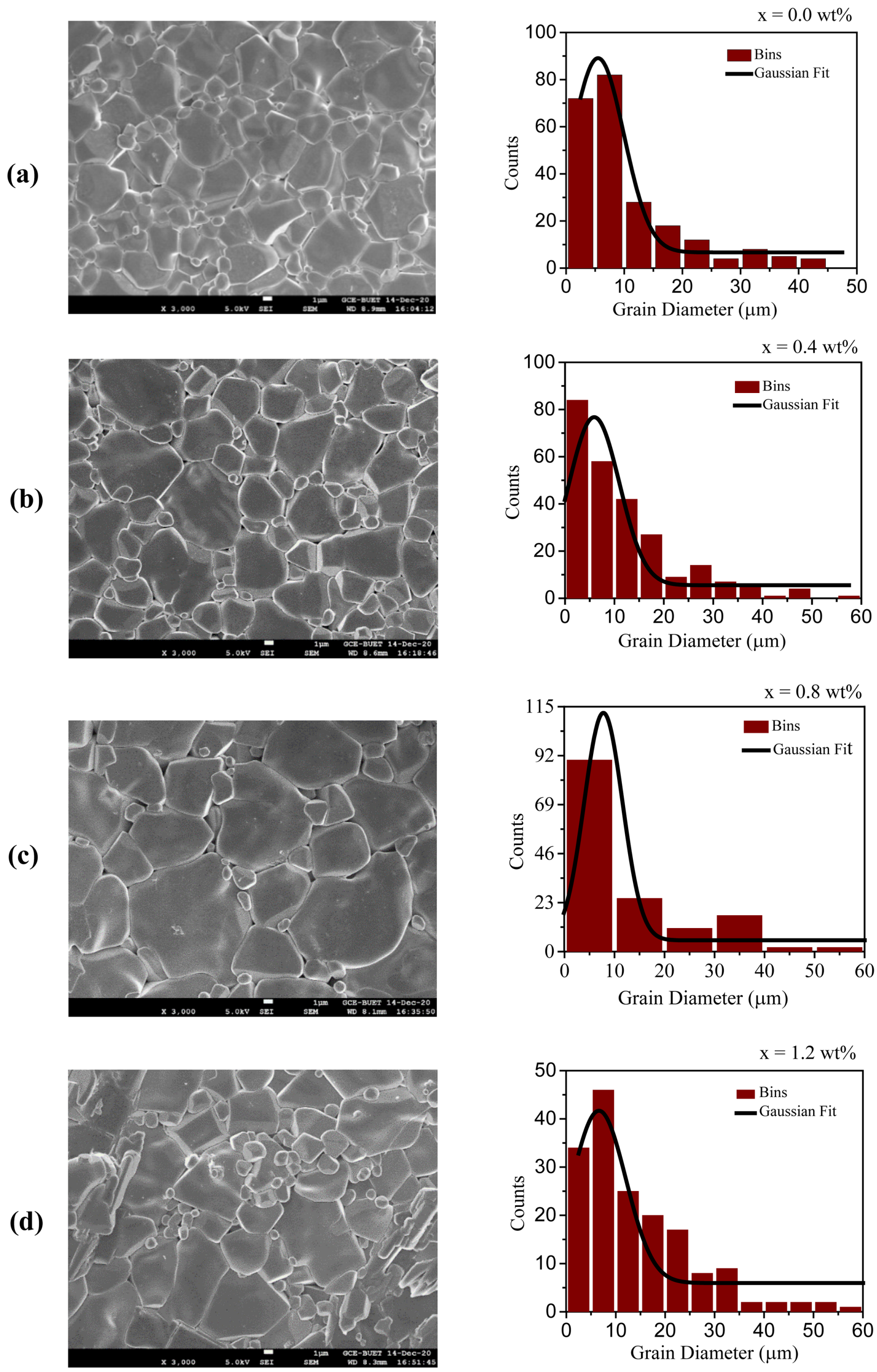

Fig. 3. (Color online) FESEM images of Li-Zn ferrites with various V_2O_5 (a) 0.0 (b) 0.4 (c) 0.8 and (d) 1.2 wt.%.

wt.% V_2O_5 content. This decrease of magnetization at more than 0.8 wt.% V_2O_5 content could be happened due to the presence of excessive non-magnetic V_2O_5 content [21]. The moderate/optimum content of V_2O_5 can alter the densification as well as promote the grain growth in the sintering process. This may lead to the increase of magnetization with V_2O_5 content. However, V_2O_5 acts inversely as a gain growth inhibitor when it is higher than 0.8 wt.%. This may lead to the decrease of magnetization at higher V_2O_5 addition due to the dilution effect of a non-magnetic V_2O_5 content.

Fig. 6 shows the variation of the real part of the initial

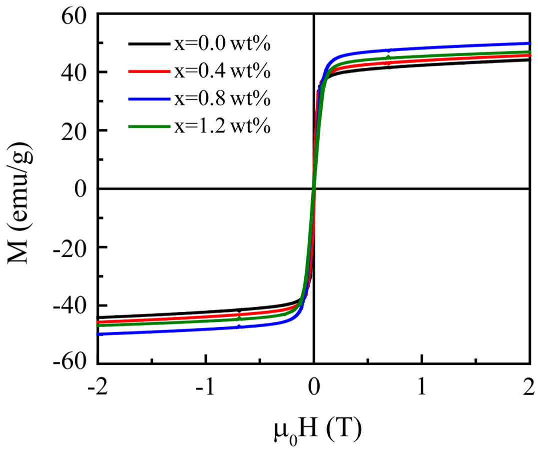

Fig. 4. (Color online) Magnetic hysteresis (*M-H*) curve of V_2O_5 added Li-Zn ferrites.

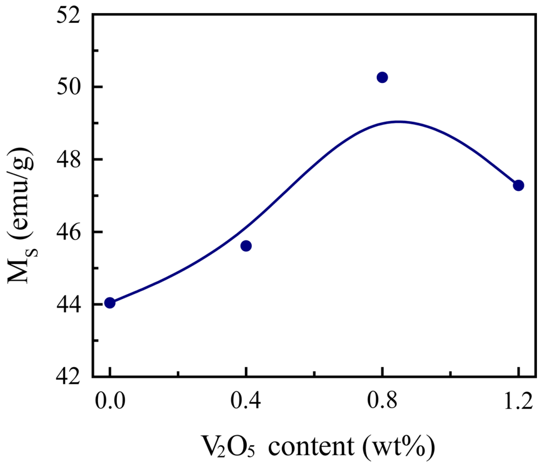

Fig. 5. (Color online) Variation of M_S of Li-Zn ferrites with different V_2O_5 contents.

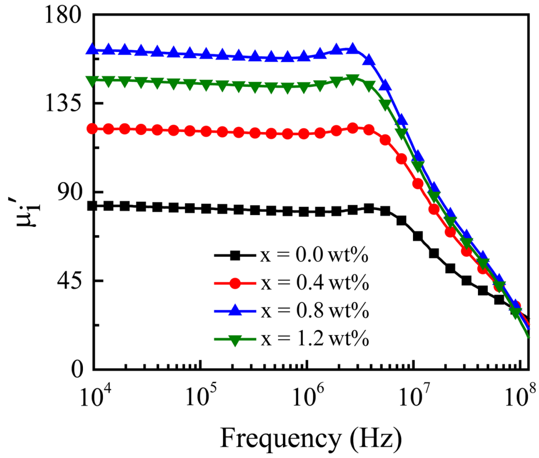

Fig. 6. (Color online) Variation of μ_i' as a function of applied frequency.

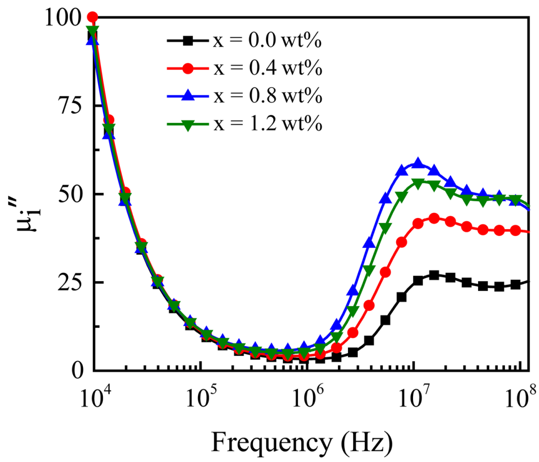

Fig. 7. (Color online) Variation of μ_i'' as a function of applied frequency.

permeability (μ_i') with the applied frequency for various amounts of V_2O_5 added Li-Zn ferrites. It is observed that μ_i' remains almost constant up to some critical frequency characterized by the onset of resonance, after a small rise, then curves drop at a higher frequency, while the imaginary part of the initial permeability (μ_i'') gradually increased with the applied frequency and shows a broad maximum in the higher frequency region as shown in Fig. 7. This behavior is shown for all the samples. This is called ferrimagnetic resonance [22, 23]. It is clearly observed that the value of μ_i' increases with the addition of V_2O_5 up to 0.8 wt.%. The increase of μ_i' could be ascribed to the increase in grain size and densification of the samples [24]. It is also observed that the resonant frequencies are shifted towards the lower frequency with the addition of V_2O_5 which is following the Snoek's relation [25]. However, μ_i' is reduced for 1.2 wt.% V_2O_5 which may be related to the reduction of density or the subsequent increase of porosity along with the reduction of the grain size.

4. Conclusion

In this study, the compactness of Li-Zn ferrites is obtained with the addition of V_2O_5 sintered at 1050 °C. The XRD patterns indicate that the involvement of V_2O_5 additive has no influence on the crystal structure. The microstructural study has been shown that the grain growth of Li-Zn ferrites is strongly dependent on the amount of V_2O_5 addition. The average grain size is found to larger at 0.8 wt.% V_2O_5 content, which could be attributed to the densification of the sample due to the role of V_2O_5 as the sintering aid. The saturation magnetization and initial permeability are found to larger for 0.8 wt.% V_2O_5 addition. It is inferred that an optimum amount of V_2O_5 additive can play a vital role for improving the magnetic properties of Li-Zn ferrites.

Acknowledgement

The authors are thankful to the Materials Science Division, Atomic Energy Center Dhaka-1000, and Department of Nanomaterials and Ceramic Engineering, Bangladesh University of Engineering and Technology, Dhaka-1000 for their support to carry out this research work.

References

[1] Y. Gao, Z. Wang, R. Shi, J. Pei, H. Zhang, and X. Zhou, J. Alloys Compd. **805**, 934 (2019).
[2] Y. Gao, Z. Wang, J. Pei, and H. Zhang, J. Alloys Compd. **774**, 1233 (2019).
[3] A. V. Anupama, V. Rathod, V. M. Jali, and B. Sahoo, J. Alloys Compd. **728**, 1091 (2017).
[4] V. Rathod, A. V. Anupama, V. M. Jali, V. A. Hiremath, and B. Sahoo, Ceram. Int. **43**, 14431 (2017).
[5] S. A. Saafan, S. T. Assar, B. M. Moharram, and M. K. E. Nimr, J. Magn. Magn. Mater. **322**, 628 (2010).
[6] I. Soibam, S. Phanjoubam, and C. Prakash, J. Magn. Magn. Mater. **321**, 2779 (2009).
[7] T. Nakamura, T. Miyamoto, and Y. Yamada, J. Magn. Magn. Mater. **256**, 340 (2003).
[8] M. Samir Ullah, M. Firoz Uddin, A. A. Momin, and M. A. Hakim, Mater. Res. Express **8**, 016102 (2021).
[9] H. Bahiraei and C. K. Ong, J. Mater. Sci.: Mater. Electron. **32**, 26967 (2021).
[10] Y. Yang, J. Li, H. Zhang, G. Wang, G. Gan, and Y. Rao, J. Mater. Sci.: Mater. Electron. **31**, 12325 (2020).
[11] F. Xie, L. Jia, F. Xu, G. Gan, J. Li, Y. Li, Y. Li, and H. Zhang, J. Mater. Sci.: Mater. Electron. **29**, 13337 (2018).
[12] Y. Jin, H. Zhu, Y. Xu, H. Zhu, H. Zhou, and Y. Jin, J. Mater. Sci.: Mater. Electron. **26**, 2397 (2015).
[13] B. P. Rao, O. Caltun, I. Dumitru, and L. Spinu, J. Magn. Magn. Mater. **304**, 749 (2006).
[14] K. Raju, G. Venkataiah, and D. H. Yoon, Ceram. Int. **40**, 9337 (2014).
[15] J. Du, G. Yao, Y. Liu, J. Mia, and G. Zu, Ceram. Int. **38**, 1707 (2012).
[16] R. Lebourgeois, S. Duguey, J. P. Ganne, and J. M. Heintz, J. Magn. Magn. Mater. **312**, 328 (2007).
[17] B. D. Cullity, "Elements of X-ray Diffraction" Addison-Wesley Publishing Company, Inc., MA, USA.
[18] X. Wang, K. Yin, T. Cao, Y. Liao, Z. Wang, Q. Kou, and D. Cheng, J. Alloys Compd. **885**, 160983 (2021).
[19] M. A. Darwish, S. A. Saafan, D. E. Kony, and N. A. Salahuddin, J. Magn. Magn. Mater. **385**, 99 (2015).
[20] X. Wang, D. Zhang, G. Wang, L. Jin, J. Li, Y. Liao, H. Zhang, and S. Wang, Ceram. Int. **46**, 10652 (2020).
[21] F. Xu, X. Shi, Y. Liao, J. Li, and J. Hu, Ceram Int. **46**, 14669 (2020).
[22] Y.-P. Fu and S.-H. Hu, Ceram. Int. **36**, 1311 (2010).
[23] S. Manjura Hoque, M. Samir Ullah, F. A. Khan, M. A. Hakim, and D. K. Saha, Physica B **406**, 1799 (2011).
[24] S. Manjura Hoque, Md. Amanullah Choudhury, and Md. Fakrul Islam, J. Magn. Magn. Mater. **251**, 292 (2002).
[25] J. L. Snoek, Physica **14**, 207 (1948).